SINAI International Scientific Journal (SISJ)

Volume 2, Issue 1, July 2025

In Silico Target Fishing, Molecular Docking and In vitro Cytotoxicity Evaluation of a New Isolated Compound Sprageuanone from Ficus sprageuana

Hatem S. Abbass[1,2], Abd El-Salam I. Mohammed[1], Ehab A. Ragab[1], Mohamed T. Elsaady[3], Ahmed R. Elaraby[3] and Atef A. El-Hela[1]*

[1]*Department of Pharmacognosy and Medicinal Plants, Faculty of Pharmacy, Al-Azhar University (Boys), Cairo 11884, Egypt.*

[2]*Department of Pharmacognosy, Faculty of Pharmacy, Sinai University - Kantara Branch, Ismailia 41636, Egypt.*

[3]*Department of Medicinal Chemistry, Faculty of Pharmacy, Sinai University - Kantara Branch, Ismailia 41636, Egypt.*

**Corresponding author*

Correspondence:

Hatem Sameir Abbass
Email: hatem.samir@su.edu.eg

Citation:

Abbass, H.S, Mohammed, A.I, Ragab, E.A, Elsaady, M.T, Elaraby, A.R, and El-Hela, A.A "*In silico* target fishing, molecular docking and *in vitro* cytotoxicity evaluation of a new isolated compound Sprageuanone from *Ficus sprageuana*", SINAI International Scientific Journal (SISJ), vol. 2, Issue 1, pp. 5-20, 2025

Received: 10 September 2024

Accepted: 4 January 2025

ABSTRACT

Objective: *Ficus sprageuana*, which is cultivated in Egypt, has a probable cytotoxic potential. However, limited studies have been conducted to explore this compound. **Methodology:** The isolation of the newly identified compound, in conjunction with three C-glycoside compounds, was executed utilizing a VLC chromatographic technique, followed by several silica gel column purifications and final refinement through gel permeation. The elucidation of the structures of the isolated compounds, namely sprageuanone (1), isovitexin (2), orientin (3), and isoorientin (4), was performed through 1D-NMR, 2D-NMR, mass spectrometry, UV, and IR spectral analysis. The *in silico* and *in vitro* investigations collectively substantiate the cytotoxic potential of the newly isolated and characterized compound sprageuanone. A target fishing approach was employed for the identification of an optimal target for molecular docking assessment. The outcomes of the target fishing indicated Mitogen-activated protein kinase to be the most suitable target.

Results: The molecular docking results validated a moderate *in vitro* cytotoxicity activity against colon carcinoma (HCT-116 cell lines), with IC_{50} value of 4.93µg/ml, in comparison to the standard Vinblastine, which exhibited IC_{50} value of 2.38µg/ml, while the most favorable docking score was recorded at -9.141.

Conclusion: In conclusion of the study, it can be posited with considerable confidence that sprageuanone represents an exceptionally promising and viable scaffold that has significant potential for the development of novel derivatives specifically aimed at combating colon cancer effectively.

KEYWORDS: Cytotoxicity, 1D & 2D NMR, Docking, Ficus sprageuana, Target fishing.

1. INTRODUCTION

Ficus sprageuana Mildbr. & Burret leaves (FSL), cultivated in Egypt, show promise for cytotoxic potential, yet research on them remains limited. The existing literature highlights the broader anticancer capabilities of various *Ficus* species, suggesting a need for further exploration of FSL [1]. Previous chromatographic separation methodologies afforded the isolation of 13 compounds from both ethyl acetate and *n*-butanol fractions of FSL [2-4]. Spectroscopic analysis confirmed that the isolated compounds were rhamnazin, rhamnocitrin, kaempferol, epiafzelechin, epicatechin, (-)-afzelechin-(4α→8)-epicatechin, catharticin, kaempferol-3-*O*- rhamninoside, syringic acid, *p*-coumaric acid, 3`,5`-*O*-dicaffeoylquinic acid, orientin, and 8-methoxy kaempferol-3-*O*-[α-L-rhamnopyranosyl-(1→2)-*β*-D-glucopyranoside [2-4]. The results of total phenolic and flavonoid contents measured in FSL showed high

Online ISSN: 3009-7800

Print ISSN: 3009-6324

concentration in both phenolic and flavonoid compounds by values of 136 and 100 mg/g, respectively [5]. HPLC investigation allowed the identification and quantification of the four compounds, namely gallic acid, chlorogenic acid, caffeic acid, and rutin; chlorogenic acid and rutin were the most abundant phenolic compounds. HPLC–ESI/MS spectrometric analysis of FSL revealed the identification of 37 phenolic compounds [2]. Biological screening of FSL assessed its efficacy in managing eczema, nephrotoxicity, and hepatoprotection [2-4]. The anti-eczematic effects of various fractions were evaluated in mice. All fractions (methanol, ethyl acetate, and *n*-butanol) demonstrated significant anti-eczematic properties. The ethyl acetate fraction exhibited the highest activity [4]. Consequently, its efficacy was tested in human volunteers, outperforming 0.1% mometasone furoate for chronic eczema treatment [4]. Both the 70% alcohol extract and ethyl acetate fraction exhibited cytotoxicity against the MDBK cell line, with the ethyl acetate fraction being the most effective. The ethyl acetate fraction and (-)-afzelechin-(4α→8)-epicatechin displayed minimal cytotoxicity against MCF-7 cells compared to vinblastine [3]. Administration of the FSL hydroalcoholic extract improved kidney function by reducing several biomarkers of injury and inflammation. Additionally, it mitigated oxidative stress, enhancing antioxidant levels and ameliorating renal histopathology [2]. The hepatoprotective effects of FSL against cholestatic liver diseases were attributed to modulation of NF-κB and FXR signaling pathways. The (-)-afzelechin-(4α→8)-epicatechin that is taken from FSL inhibited HepG2 tumor cell proliferation, albeit less effectively than doxorubicin. The acute oral toxicity assessment of FSL hydroalcoholic extract revealed no adverse effects at doses up to 2 g/kg [3, 5].

Target fishing, which involves finding biological targets for bioactive molecules, is a crucial technique in contemporary drug development. Because it links phenotypic findings with molecular processes, this approach has acquired a lot of momentum and improved our knowledge of how medications function and may produce adverse effects. Drug discovery has historically been mostly dependent on empirical testing and coincidental discoveries, which has hampered our understanding of the molecular mechanisms behind these medications. Nonetheless, target fishing has developed into a more methodical and trustworthy approach thanks to developments in genomics, proteomics, and bioinformatics [6, 7]. Finding the profiles of interactions between tiny compounds and biological macromolecules, mostly proteins, is the fundamental idea behind target fishing. Finding novel therapeutic targets and repurposing current medications depend on this approach. With the use of chemical proteomics, high-throughput screening, and computer algorithms, scientists are now able to accurately and efficiently anticipate and confirm drug-target interactions. This lowers the possibility of negative medication responses and unsuccessful treatment outcomes while accelerating the drug development process [6, 7]. Furthermore, target fishing methods have greatly improved with the integration of artificial intelligence and machine learning. Large datasets may now be analyzed because of these technologies. That makes patterns and connections that were previously hard to find visible. As a result, target fishing is now a vital tool in drug discovery, enhancing the work being done in precision medicine and systems biology. In this study, we used *in silico* target fishing tools to search for biological targets for our compounds [6, 7].

The aim of the study was to isolate new compounds from FSL while assessing previously unexamined cytotoxic properties through both *in vitro* and *in silico* methodologies. The result was the isolation and characterization of four distinct compounds; one of these

SINAI International Scientific Journal (SISJ), 2025, 2(1)
Online ISSN: 3009-7800
Print ISSN: 3009-6324

exhibited properties were indicative of a potential lead compound for anti-colon cancer applications.

2. METHODOLOGY

2.1. Plant Material

Ficus sprageuana Mildbr. & Burret leaves (FSL) were collected from Orman Garden in March 2015. The identification of the plant was kindly done by Dr. Mohammed El-Gebaly, National Research Institute, Dokki, Giza, Egypt. A voucher specimen {FSL-01} is available in the Pharmacognosy and Medicinal Plants Department, Faculty of Pharmacy, Al-Azhar University, Cairo, Egypt.

2.2. Extraction and Isolation of Pure Compounds

Air-dried powder of FSL (1 kg) was subjected to exhaustive extraction by percolation with 70% MeOH (3 x 3L). The combined methanolic extracts were concentrated under vacuum at 40°C to dryness. The concentrated methanolic extract was subjected to Vacuum Liquid Chromatography (VLC) to afford 5 fractions (A, B, C, D, and E). A series of column chromatography was used to afford four compounds demonstrated in Scheme 1. Compound (1) (55 ml) was obtained from fraction A (96 g). Compound (2) (32 mg), and compounds (3, 4) (18 mg) isolated as a mixture of Wessely–Moser [8] from fraction C (149 g) in accordance with scheme 1. Stationary phases used were silica gel (Si gel 60, Merck) and Sephadex LH20 (Pharmacia). All solvents and mobile phases were purchased from Sigma Company.

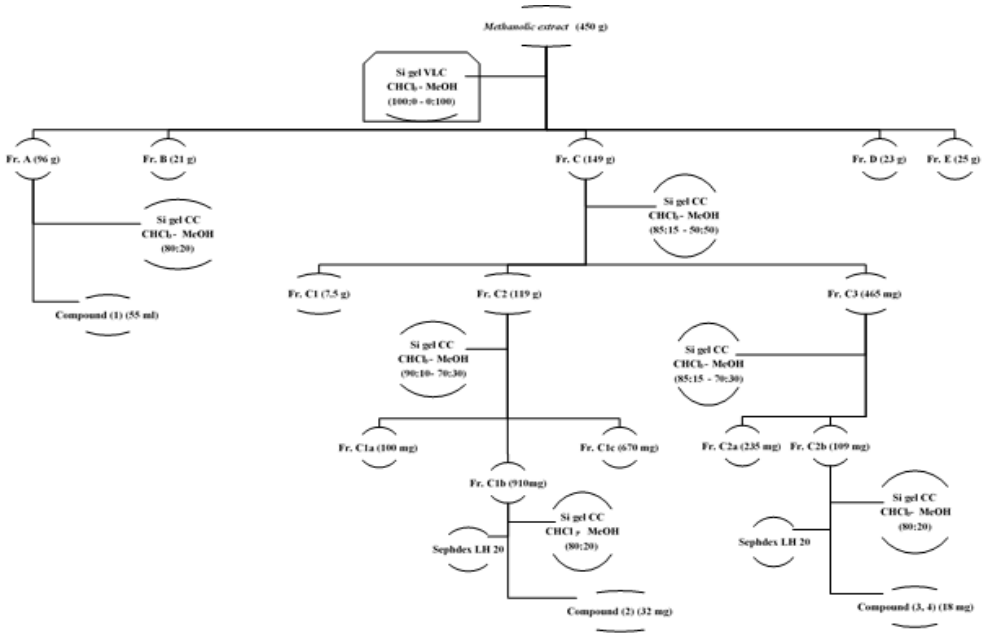

Scheme 1: Isolation of compounds (2 - 4) from methanolic extract of FSL

2.3. Structural Elucidation

NMR spectra were recorded on Bruker spectrometer operating at (400 MHz for ^{1}H and 100 MHz for ^{13}C) and were calibrated in parts per million (ppm) of downfield from

Online ISSN: 3009-7800
Print ISSN: 3009-6324

tetramethylsilane (TMS) as an internal standard. Compound (1) was measured in $CDCl_3$ while compounds (2 - 4) were measured in DMSO-d_6. Resonances are given in δ ppm (TMS, δ 0.0) and the following abbreviations have been used: s; singlet, d; doublet, t; triplet, m; multiplet, brs; broad singlet, *J*; coupling constant in Hertz (Hz). The analysis was done at the NMR unit, Faculty of Pharmacy, Cairo University, Egypt. EI-MS was carried out on VG Micromass 165 spectrometer at 18, 35 or 70 eV. with inlet temperatures between 180-240 °C. ESI-MS was carried out on a XEVO TQD triple quadruple instrument (Waters Corporation, Milford, MA 01757, USA) mass spectrometer. Pye Unicam spp. A1750 spectrophotometer and Nicolet 205 FT IR spectrophotometer connected to a Hewlett-Packard Color Pro. Plotter were used for UV and IR determination, respectively.

2.4. *In Silico* Studies

Target Fishing

Computational target fishing has been performed using PharmMapper which is an online platform designed to help researchers find potential drug targets by matching the features of a query compound with a large database of pharmacophore models. PharmMapper had over 23,000 pharmacophore targets, sourced from crystal structures with detailed annotations about their associated proteins. In PharmMapper, the fit score and Z-score are used to evaluate and rank pharmacophore-based interactions to identify potential drug targets. The fit score in PharmMapper is a measure of how well a query compound matches a specific pharmacophore model. It represents the quality of alignment between the compound's features and the pharmacophore's defined features, such as hydrogen bond donors/acceptors, hydrophobic regions, aromatic rings, etc. The fit score takes into consideration both geometric and chemical properties to evaluate the compatibility of the query compound with the pharmacophore model [9]. The fit score is typically calculated based on the overlap and alignment between the query compound's features and the corresponding features of a pharmacophore model. Higher fit scores indicate better alignment and potential interactions between the compound and the pharmacophore. The Z-score in PharmMapper is a statistical measure used to assess the significance of the fit score compared to a distribution of fit scores. It helps determine whether the observed fit score is meaningful by comparing it against a reference distribution, usually derived from random pharmacophore matches. As for calculations, The Z-score is calculated by taking the difference between the observed fit score and the mean of the reference distribution, and then dividing by the standard deviation of the distribution. Mathematically, it is represented as:

$$Z = (Fit\ Score - \mu) \,/\, \sigma \qquad (1)$$

Where μ is the mean of the reference distribution, and σ is the standard deviation. Higher Z-scores indicate that the fit score is significantly different from the expected random matches, suggesting that the interaction is likely meaningful. Together, the fit score and Z-score help rank the potential drug targets identified through reverse pharmacophore matching. A high fit score indicates a strong match between the query compound and a pharmacophore model, while a high Z-score suggests that this match is statistically significant, reducing the

Online ISSN: 3009-7800
Print ISSN: 3009-6324

likelihood of random or spurious interactions. Researchers use these scores to identify and prioritize promising drug targets for further analysis and drug development [10, 11].

Docking

After target fishing, the top 5 targets were selected to perform docking against our ligand. Protein preparation was done by the "make receptor" unit of the OpenEye suite, which quickly prepared the protein, including protonation of the 3D structure to enhance H-bonding network, and energy minimization has been done through the "make receptor" unit automatically. The ligand was prepared before docking, using OpenEye toolkit "OEchem Toolkit 4.0.0.3". Minimizing of compounds energy was employed via the forcefield "Amber: 10EHT" at a 0.01 RMSD gradient. The remaining parameters were maintained at default settings. One protonation state was made at pH 7.0 and all possible conformers were retained for each molecule using Omega version 5.1.0.0 and only the pose with the best score was selected by the docking program FRED 2023.2.3 version. The top 5 targets were selected to perform docking against our ligand. Protein preparation was done by the "make receptor" unit of OpenEye suit quick preparation to the protein including protonation of 3D structure for improving H-bonding network and energy minimization has been done through "make receptor" unit automatically. The ligand was prepared before docking using OpenEye toolkit "OEchem Toolkit 4.0.0.3". Minimizing of compounds energy was employed via forcefield "Amber: 10EHT" at a 0.01 RMSD gradient. The remaining parameters were maintained at default settings. One protonation state was made at pH 7.4 and all possible conformers were retained for each molecule using Omega version 5.1.0.0 and only the pose with the best score was selected by the docking program FRED 2023.2.3 version. FRED uses *Chemgauss 4* scoring function which is a state of art scoring function, the docking scores were visualized using VIDA 5.5.0.3 from OpenEye suit [12, 13].

Cytotoxic Activity

3.1.1.1.Sample Preparation

Various concentrations (50, 25, 12.5, 6.25, 3.125 and 1.56μg/ml) were prepared for compound (1) isolated in accordance to Scheme. 1.

3.1.1.2.Cytotoxicity Evaluation using Viability Assay (MTT test):

In this study, the cytotoxic activity of the newly isolated compound sprague anone against the human colonic epithelial carcinoma (HCT-116 cell lines) was evaluated by determining the effect of the test samples on cell morphology and cell viability of HCT-116 cell lines. A placebo-controlled trial comparing the compound with Vinblastine (obtained from the Regional Center for Mycology and Biotechnology, Al-Azhar University**)** as a positive control was done [3, 14]. The viable cells yield was determined by a colorimetric method, and the cytotoxic activity of the samples was determined by the mean percent inhibition of the tumor cells remaining after the treatment by the following formula:

$$(ODt / ODc) \times 100\% \text{ [15]} \qquad (2)$$

Where, ODt and ODc are the optical densities of wells with treated and untreated cells, respectively. The half maximal inhibitory concentration (IC_{50}) was determined using GraphPad Prism software (San Diego, CA. USA).

SINAI International Scientific Journal (SISJ), 2025, 2(1)
Online ISSN: 3009-7800
Print ISSN: 3009-6324

3. RESULTS AND DISCUSSION

3.1. Structural Elucidation of Isolated Compounds

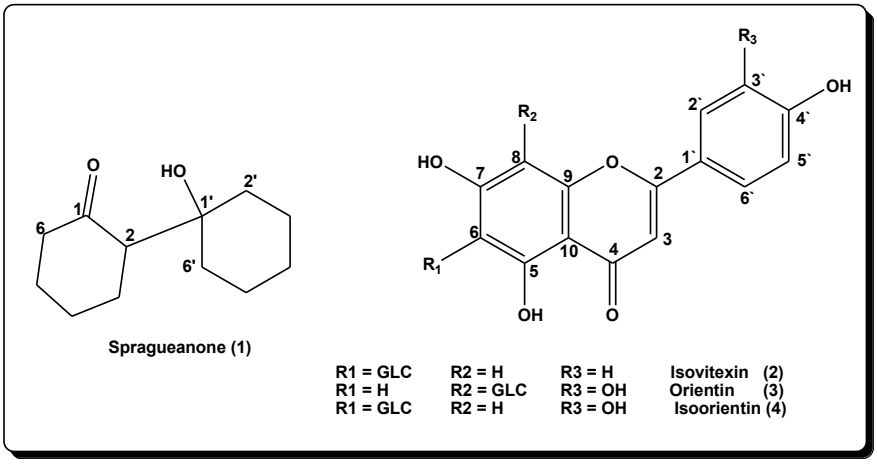

Figure 1: Chemical structures of isolated compounds

Compound (1) (Fig. 1) was obtained as a yellow oil with R_f value of 0.31 on a TLC plate using pet ether-EtOAc (95:5) as a developer. The IR spectrum displayed a characteristic cyclohexanone carbonyl group at 1697 cm^{-1}, a hydroxyl group at 3550 cm^{-1} and methine groups at 2930 and 2855 cm^{-1} [16]. The EI-MS (Figure 2) of compound (1) showed a molecular ion peak at *m\z* 196 $[M]^+$, which is presumably consistent with the molecular formula $C_{12}H_{20}O_2$. This molecular formula implied 3 degrees of unsaturation; two of them can be assigned to the dicyclic system and one degree of unsaturation is due to one carbonyl group [17]. Three characteristic fragment ions at *m\z* 179 $[M\text{-}OH]^+$, *m\z* 97 $[Cyclohexenone]^+$ and *m\z* 99 $[Cyclohexanol]^+$ were observed. Careful inspection of the 1D- and 2D-NMR data indicated that compound (1) is composed of a cyclohexanone ring attached to a cyclohexanol ring through a C-C bond. The identification of all ^1H and ^{13}C NMR signals of compound (1) was based on a combination of COSY, HSQC, and HMBC experiments (Table 1 and Figs. 3-7). Starting from the more downfield proton, all the hydrogens within each spin system were assigned using COSY spectrum [18]. On the basis of the assigned proton signals, an HSQC experiment then gave the corresponding carbon assignments, and these were further confirmed by an HMBC experiment [19]. In the ^1H NMR spectrum, the double-doubles at δ 2.33 (J = 5.0, 12.0 Hz, H-2) and a triplet-like at δ 2.27 (J = 4.9 Hz, $H_{a,b}$-6) were assigned to the protons that are adjacent to the carbonyl group as indicated from their chemical shift values and their splitting pattern [20, 21]. Additionally, these protons, H-2 and $H_{a,b}$-6 were correlated only with $H_{a,b}$-3 (δ 1.52, 2.13) and $H_{a,b}$-5 (δ 1.56, 2.0) as shown in the COSY spectrum, respectively. The ^{13}C-APT NMR spectrum displayed 12 signals, from which two signals were attributed to one keto-carbonyl carbon at δ 216.26 (C-1) and one oxygenated quaternary carbon at δ 72.13 (C-1`) as well as one methine carbon signal at δ 58.80 (C-2) [21]. The remaining signals were attributed to nine methylene groups at δ 21.30 to δ 43.72 (C-3 to C-6 and C-2` to C-6`). The $C_2$-$C_{1`}$ connectivity between the two rings was confirmed by the clearly observed HMBC cross-peak from the correlation of H-2 (δ 2.33) of the cyclohexanone ring with C-1` (δ 72.13) of the cyclohexanol ring. From the above data, the structure of compound (1) was established as 2-

SINAI International Scientific Journal (SISJ), 2025, 2(1)
Online ISSN: 3009-7800
Print ISSN: 3009-6324

(1`-hydroxycyclohexyl) cyclohexanone (*Spargueanone*) and confirmed by comparison with data of nearly similar compounds [22]. *Spargueanone* (Fig. 1) was isolated for the first time from nature.

Table 1: 1D- and 2D-NMR spectral data of compound (1) (*$CDCl_3$*, 400 and 100 MHz)

Position	^{1}H (*J* in Hz)	^{13}C-APT	COSY	HMBC
1	-	216.26, C	-	-
2	2.33, dd, 12.0, 5.0	58.80, CH	H-3a, b	C-3, 1`
3a 3b	1.52, m 2.13, m	28.94, CH_2	H-2, 3b, 4b H-2, 3a, 4a	-
4a 4b	1.55, m 1.84, m	25.39, CH_2	H-4b, 5b H-3a, 4a, 5a	-
5a 5b	1.56, m 2.00, m	28.19, CH_2	H-4b, 5b, 6 H-4a, 5a, 6	-
6	2.27, t, 4.9	43.72, CH_2	H-5a, b	C-4, 5
1`	-	72.13, C	-	-
2`a 2`b	1.35, m 1.57, m	35.94, CH_2	H-3` H-3`	C-6`
3`	1.61, m	21.58, CH_2	H-2`a, 2`b, 4`a	-
4`	1.09, m 1.51, m	25.81, CH_2	H-3`, 4`b, 5`a H-4`a	-
5`	1.34, m 1.60, m	21.30, CH_2	H-4`a, 5b, 6`b H-4`a, 5`a	C-6`
6`	1.20, m 1.61, m	33.16, CH_2	H-5`b, 6`b H-5`a, 6`a	C-5`
OH	3.72, brs	-	-	-

Compounds (2 – 4) (Fig.1) were isolated as yellow crystals and elucidated by ESI-MS (Figs 8, 9) and 1D- and 2D-NMR data (Table 1 and Figs. 10-15). Compound (2) was obtained as a pure single compound, while compounds (3, 4) were obtained in the form of a Wessely–Moser isomer mixture [8]. The signals of each isomer were assigned according to 1D- and 2D-NMR data; thus the same signals were observed in the ^{1}H- and ^{13}C-NMR spectra, but with slightly different chemical shifts. The signals of each isomer were selected and extracted from the ^{1}H- and ^{13}C NMR spectra, based on their correlations observed in HSQC and HMBC spectra. The HSQC experiment gave the corresponding carbon assignments on the basis of the assigned proton signals, and these were further confirmed by an HMBC experiment. Compounds (2 - 4) gave crimson red under UV (365nm), which changed to intense yellow after spraying with 2% $AlCl_3$, indicating a flavone nucleus with free 5- and 4`-hydroxyl groups [23]. The flavone nucleus of compounds (2 - 4) was further confirmed by the bathochromic shift and unchanged intensity of band I in presence of NaOMe indicated a free 4`-OH and no hydroxylation at C-3. The flavone nucleus was confirmed to be an apigenin type regarding compound (2) and a luteolin type regarding compounds (3, 4) by both UV and ^{1}H NMR spectral data [24, 25]. The free 7-OH in the three compounds was deduced from the bathochromic shift of band II after the addition of NaOAc. The bathochromic shift of band I of compounds (3, 4), after the addition of H_3BO_4 and its absence for compound (2), as well as the comparison of the spectra recorded in MeOH/$AlCl_3$ and in MeOH/$AlCl_3$ + HCl, confirmed the *ortho*-hydroxylation of ring B in compounds (3, 4) and their absence in compound (2) [23, 26]. Furthermore, the ^{1}H NMR spectrum of (2) showed an AA`BB` spin-system corresponding to the equivalent protons of ring B, while those of (3, 4) showed two different ABX spin systems

Online ISSN: 3009-7800
Print ISSN: 3009-6324

corresponding to the pair of three aromatic resonances due to the two different isomers. The ^{13}C NMR spectrum of (2) displayed 19 distinct carbon signals from which 13 carbon signals were assigned to the apigenin aglycon moiety.

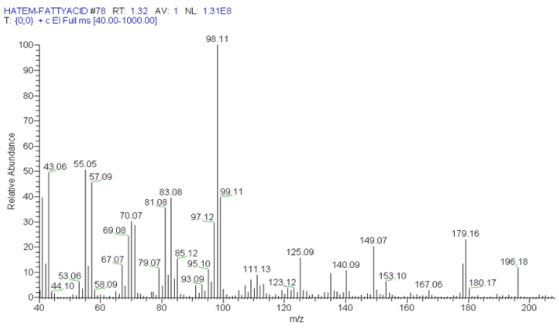

Figure 2: EI-MS spectrum of compound (1)

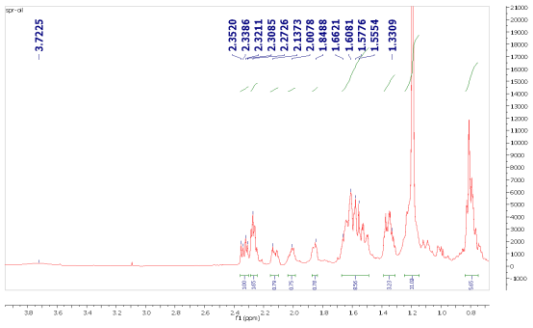

Figure 3: ^{1}H-NMR spectrum of compound (1)

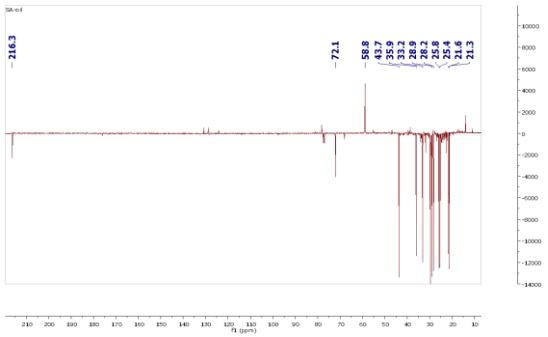

Figure 4: ^{13}C-APT NMR spectrum of compound (1)

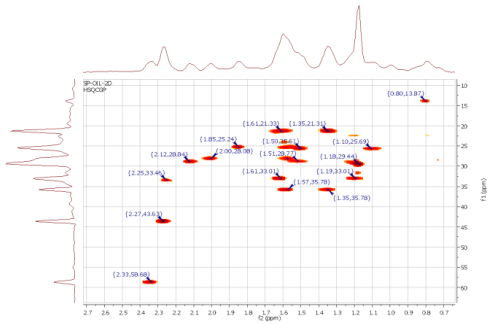

Figure 5: HSQC spectrum of compound (1)

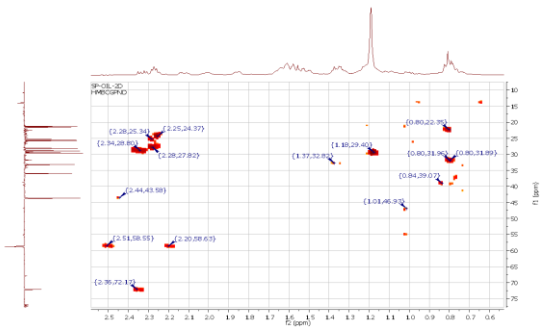

Figure 6: HMBC spectrum of compound (1)

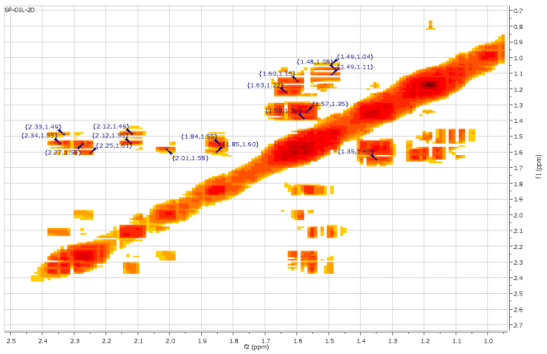

Figure 7: COSY spectrum of compound (1)

The ^{13}C NMR spectrum of compounds (3, 4) displayed 42 distinct carbon signals from which 30 carbon signals were assigned to the two luteolin aglycons. The remaining six oxygenated aliphatic carbon signals in case of (2) and the remaining twelve carbon signals in case of (3, 4) were assigned to the glucose moieties. Free glucoses were obtained up on oxidative hydrolysis of compounds (3, 4) using ferric chloride [27] as confirmed by TLC examination [$CHCl_3$-MeOH-H_2O, (61:32:7)], while no free sugars were formed up on normal acid hydrolysis confirmed the C-glycoside nature of compounds (3, 4) [28]. Furthermore, ^{1}H NMR spectra of (2 - 4), also exhibited three anomeric proton signals resonated at δ 4.59 (1H,

Online ISSN: 3009-7800
Print ISSN: 3009-6324

d, J = 9.8 Hz), 4.67 (1H, d, J = 9.8 Hz), and 4.56 (1H, d, J = 9.7 Hz) were assigned to the three glucose moieties for (2 - 4), respectively. The large coupling constant of the anomeric proton signals suggested that the configuration of the glucose was in the *β*-form [29]. The absence of one methine proton and carbon signal due to ring-A of each compound, along with the presence of a quaternary carbon signal indicated ring-A substitution. The C-glycosylation of flavonoids shifts the signal of the glycosylated carbon downfield by 8.6-10.2 ppm and the *ortho*-related carbons upfield by 0.1-1.4 ppm, while other carbon signals are not significantly affected [30]. Therefore, the downfield shift of C-6 and the upfield shift of C-7 for compounds (2, 4) indicated that the glucose substitution in both compounds occurred at C-6. The downfield shift of C-8 and the upfield shift of C-7 for compound (**3**) indicated that the glucose substitution in both compounds occurred at C-8 as compared to those of luteolin and apigenin. The IR spectra of (2) and (3, 4) showed resonances at 3399 and 3400 cm^{-1} corresponding to hydroxyl groups, respectively. The carbonyl groups and the aromatic rings were indicated from the absorption bands at (1650 and 1658 cm^{-1}) and (1492–1597 cm^{-1}), respectively [31]. The ESI-MS of compound (2) showed a pseudomolecular ion peak corresponding to $[M+H]^+$ at *m/z* 433, which is compatible with the molecular formula $C_{21}H_{20}O_{10}$.

Table 2: 1D and 2D-NMR spectral data of compounds (2 - 4) (DMSO-d_6, 400 and 100 MHz)

	Isovitexin		Orientin			Isoorientin		
Position	$^1H^*$	^{13}C	$^1H^*$	^{13}C	HMBC	$^1H^*$	^{13}C	HMBC
1			-	-	-	-	-	-
2	-	164.01	-	164.32	-	-	164.32	-
3	6.79, s	103.25	6.64, s	102.56	C-2, 4, 10, 1`	6.66, s	102.92	C-2, 4, 10, 1`
4	-	182.43	-	182.22	-	-	182.07	-
5	-	161.66	-	160.52	-	-	162.81	-
6	-	109.33	6.31, s	98.35	C-5, 7, 8, 10	-	108.96	-
7	-	163.75	-	163.55	-	-	163.87	-
8	6.53, s	94.22	-	104.68	-	6.56, s	93.74	C-6, 7, 9, 10
9	-	156.69	-	156.16	-	-	156.39	-
10	-	103.87	-	104.16	-	-	103.52	-
1`	-	121.55	-	122.12	-	-	121.56	-
2`	7.93, d, 8.7	128.95	7.39, d, 2.1	113.43	C-2, 1`, 3`, 4`, 6`	7.46, d, 1.9	114.13	C-2, 1`, 3`, 4`, 6`
3`	6.93, d, 8.7	116.47	-	145.94	-		145.97	-
4`	-	161.14	-	149.84	-	-	149.91	-
5`	6.93, d, 8.7	116.47	6.88, d, 8.1	115.95	C-1`, 2`, 3`, 4`, 6`	6.91, d, 8.4	116.31	C-1`, 2`, 3`, 4`, 6`
6`	7.93, d, 8.7	128.95	7.40, dd, 8.1, 2.1	119.12	C-2, 1`, 2`, 4`, 5`	7.52, dd, 8.4, 2.0	119.57	C-2, 1`, 2`, 4`, 5`
1``	4.59, d, 9.8	73.51	4.67, d, 9.8	73.51	C-7	4.56, d, 9.7	73.17	C-7
2``	4.05, t, 9.0	71.06	3.35, m	70.88	C-1``, 3``	4.05, m	70.32	C-1``, 3``
3``	3.30, m,	79.40	3.28, m	78.88	C-2``, 4``	3.24, m	79.10	C-2``, 4``
4``	3.21, t, 8.8	70.66	3.82, dd, 3.2, 9.3	70.98	C-3``, 5``	3.2, d, 9.4	70.75	C-3``, 5``
5``	3.15, m	82.02	3.15, m	81.69	C-1``, 3``, 4``, 6``	3.26, m	82.08	C-1``, 3``, 4``, 6``
6``	3.69, d, 11.8 3.41, m	61.93	3.46, m 3.66, m	61.63	C-4``, 5``	3.53, m 3.76, m	61.81	C-4``, 5``
5-OH	13.56, s	-	13.14, brs	-	C-5, 6, 10	13.53, brs	-	C-5, 6, 10
OH	9.33, brs	-	10.87, brs	-	-	11.06, brs	-	-
OH	8.97, brs	-	9.25, brs	-	-	9.60, brs	-	-
OH	-	-	10.01, brs	-	-	10.18, brs	-	-

SINAI International Scientific Journal (SISJ), 2025, 2(1)
Online ISSN: 3009-7800
Print ISSN: 3009-6324

The positive ESI-MS of compounds (3, 4) gave the pseudomolecular ion at *m/z* 449 $[M+H]^+$. Thus, its molecular formula was consistent with $C_{21}H_{20}O_{11}$, and by applying successively higher cone voltages, characteristic fragment ions of the C-6 and C-8 glycosides were observed at *m/z* 431 $[M+H-H_2O]^+$, *m/z* 413 $[M+H-2H_2O]^+$, *m/z* 395 $[M+H-3H_2O]^+$, *m/z* 329 $[M+H-120]^+$ and *m/z* 299 $[M+H-150]^+$ [32, 33]. From the above evidence and data, compound (2) was established as apigenin-C-6-*β*-D-glucopyranoside (isovitexin) and in good agreement with published data [34, 35]. Compounds (3, 4) were established as orientin and isoorientin isomers, at which the relative ratio found to be 3:2 by the aid of proton NMR signals intensity. Isovitexin and isoorientin were isolated before from *Ficus* genus [36, 37]. Their isolation from *Ficus spragueana* is reported as follows:

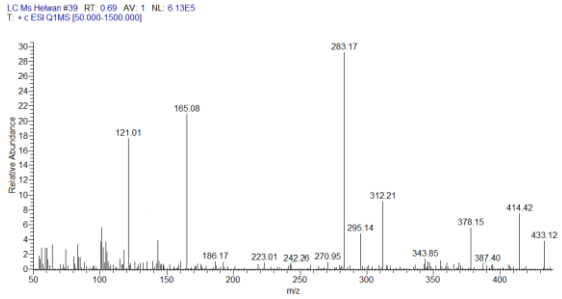

Figure 8: ESI-MS spectrum of compound (2)

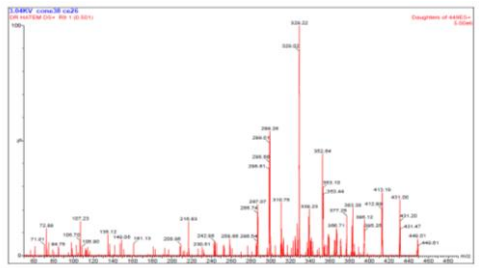

Figure 9: ESI-MS spectrum of compounds (3, 4)

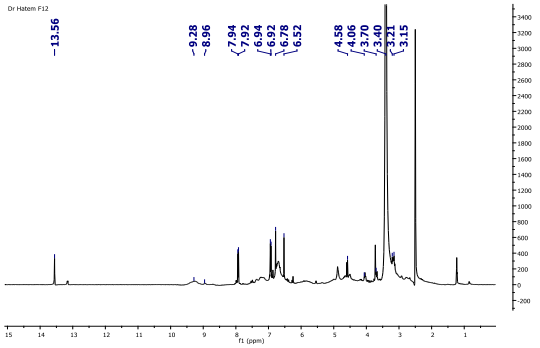

Figure 10: ^{1}H-NMR spectrum of compound (2)

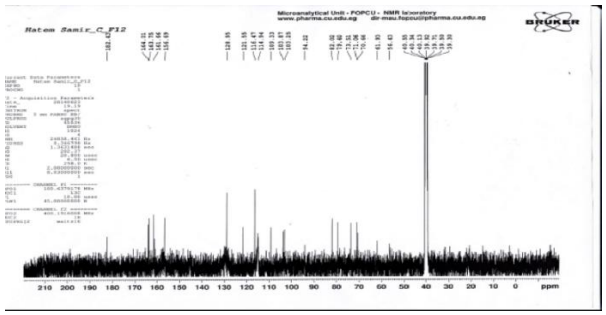

Figure 11: ^{13}C-NMR spectrum of compound (2)

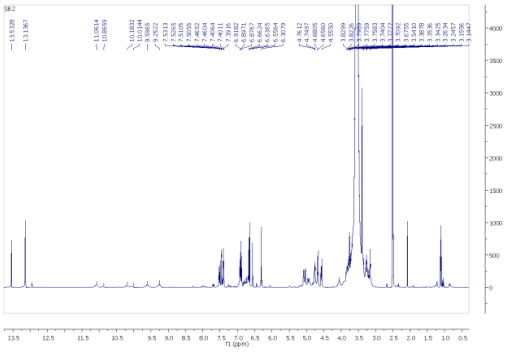

Figure 12: ^{1}H-NMR spectrum of compounds (3, 4)

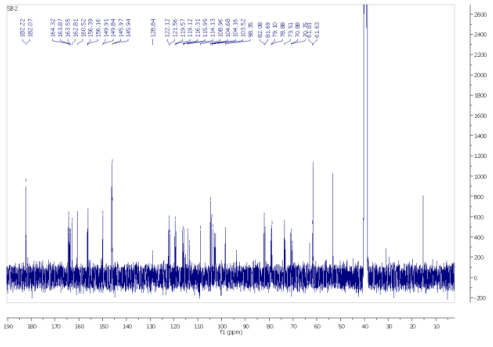

Figure 13: ^{13}C-NMR spectrum of compounds (3, 4)

SINAI International Scientific Journal (SISJ), 2025, 2(1)
Online ISSN: 3009-7800
Print ISSN: 3009-6324

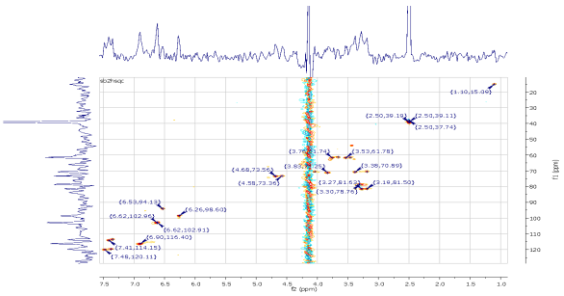

Figure 14: HSQC spectrum of compounds (3, 4)

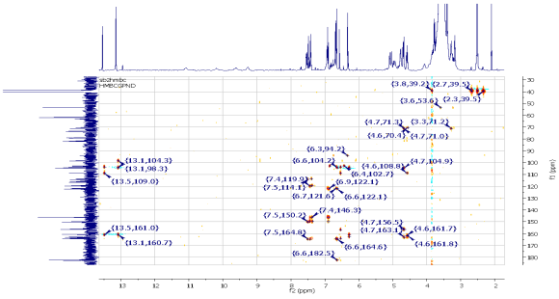

Figure 15: HMBC spectrum of compounds (3, 4)

3.2. In Silico Studies

3.2.1 Target Fishing

The target fishing results suggested Mitogen-activated protein kinase 10 as a predicted target for spargueanone docking study (Table 3).

Table 3: The top 10 predicted targets for compound (1).

Protein PDB code	Norm Fit	Z score	Name
1rs0	0.9839	2.19197	Complement factor B
1no9	0.9195	1.07178	Prothrombin
1uki	0.9184	1.0094	Mitogen-activated protein kinase 8
1pmv	0.9099	0.803171	Mitogen-activated protein kinase 10
1bm6	0.8546	0.036503	Stromelysin-1
1mx1	0.7219	1.4186	Liver carboxylesterase 1
2ohm	0.705	1.26375	Beta-secretase 1
2r3f	0.6998	1.24356	Cell division protein kinase 2
1q8m	0.6808	-1.59723	Triggering receptor expressed on myeloid cells 1
1n1m	0.6769	0.750064	Dipeptidyl peptidase 4
1s95	0.6714	0.565254	Serine/threonine-protein phosphatase 5
1w84	0.67	0.45108	Mitogen-activated protein kinase 14

3.2.2 Docking Results

The best docking score was -9.141 for the ligand with Mitogen-activated protein kinase 10 PDB code: 1PMV (25). Figure 16 represents the 2D interactions between the ligand and target protein, while Figure 17 represents the 3D docking pose for the ligand.

Online ISSN: 3009-7800
Print ISSN: 3009-6324

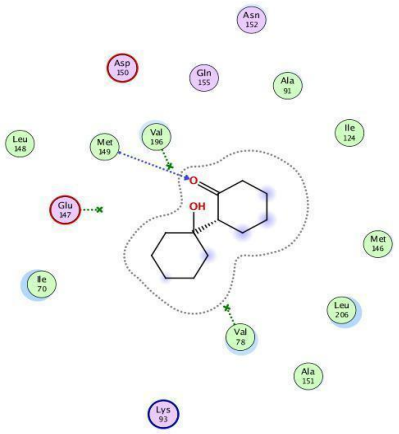

Figure 16: 2D ligand protein interaction between compound with the best docking score and Mitogen-activated protein kinase 10 PDB code: 1PMV.

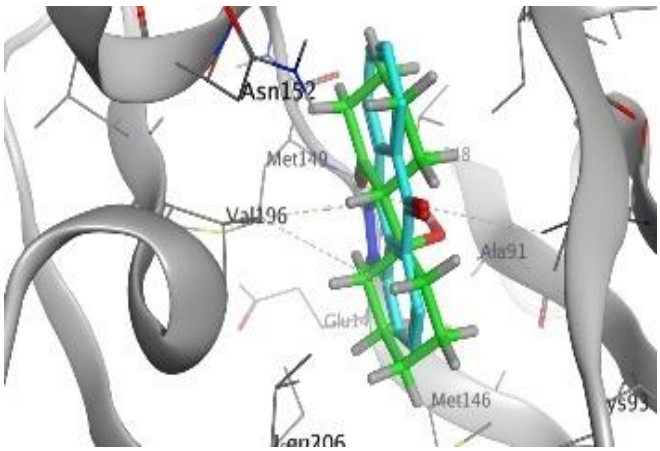

Figure 17: Superimposition between ligand and co-crystalized ligand dihydroanthrapyrazole inhibitor. The ligand with cyan color and co-crystalized ligand with green color.

3.2.3 Cytotoxic Activity Against Colon Carcinoma Cell Lines

The viability of the tested cell lines and the IC_{50} values were shown in Table 4 and Figure 18. Sprageanone exhibited moderate cytotoxic activity against colon carcinoma (HCT-116) cell lines with IC_{50} value of 4.93μg/ml compared to the standard IC_{50} value of 2.38μg/ml. Sprageanone was found to give inhibition upon the proliferation of examined colon carcinoma (HCT-116) cell lines with less potency than positive control Vinblastine [3, 38].

Table 4: Cytotoxic activity of sprageanone against colon carcinoma cell lines

Sample conc. (μg)	Sprageanone	Vinblastine[a]
50	**18.02**	**12.16**
25	**23.84**	**15.54**
12.5	**35.16**	**18.92**
6.25	**43.92**	**39.86**
3.12	**58.31**	**47.30**
1.56	**74.26**	**58.11**
0	**100**	**100**
[b]IC_{50} μg/ml	**4.93**	**2.38**

[a] *Positive control substance.*
[b] *IC_{50} is defined as the concentration that resulted in a 50% decrease in cell number*

SINAI International Scientific Journal (SISJ), 2025, 2(1)
Online ISSN: 3009-7800
Print ISSN: 3009-6324

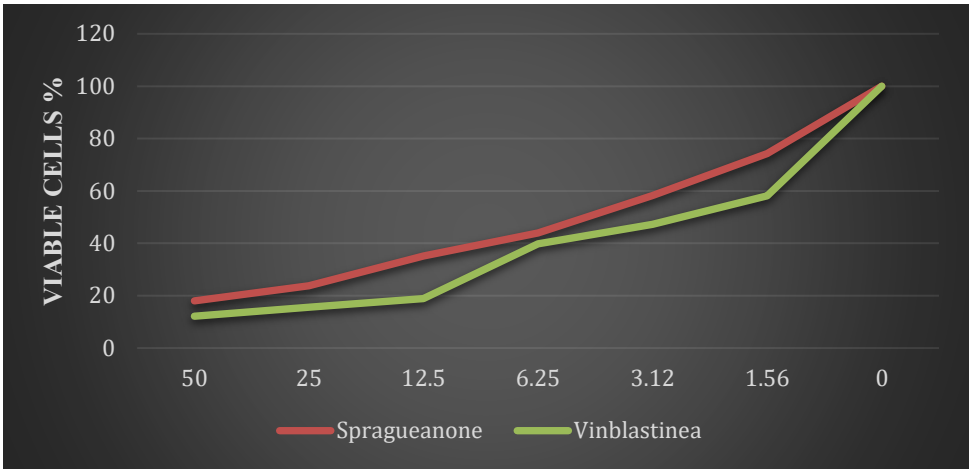

Figure 18: Cytotoxic activity of spragueanone against colon carcinoma cell lines

4. CONCLUSIONS

Phytochemical inspection of FSL provided isolation and identification of a new compound (Spragueanone) along with three C-glycoside flavones. The *in vitro* and *in silico* studies revealed that spragueanone is a promising scaffold for new anti-colon cancer derivatives.

ACKNOWLEDGEMENT

We would like to thank Dr. Mohammed El-Gebaly, National Research Institute, Dokki, Giza, Egypt for his kind identification of the plant. Also, we gratefully acknowledge the support of OpenEye for the academic licensing of their software.

CONFLICT OF INTEREST

No conflicts exist.

FUNDING

None is declared

REFERENCES

[1] Salehi B, Prakash Mishra A, Nigam M, Karazhan N, Shukla I, Kiełtyka-Dadasiewicz A, et al. Ficus plants: state of the art from a phytochemical, pharmacological, and toxicological perspective. Phytotherapy Research. 2021;35(3):1187-217. Doi: 10.1002/ptr.6884.

[2] Taher RF, Raslan MA, Masoud MA, Nassar MI, Aboutabl ME. HPLC–ESI/MS profiling, phytoconstituent isolation and evaluation of renal function, oxidative stress and inflammation in gentamicin-induced nephrotoxicity in rats of Ficus sprague ana Mildbr. & Burret. Biomedical Chromatography. 2021;35(9):e5135. Doi: 10.1002/bmc.5135.

[3] Ragab EA, Mohammed AE-SI, Abbass HS, Kotb SI. A new flavan-3-ol dimer from Ficus sprague ana leaves and its cytotoxic activity. Pharmacognosy Magazine. 2013;9(34):144. Doi: 10.4103/0973-1296.111274.
[4] Hegazy MM, Mekky RH, Afifi WM, Mostafa AE, Abbass HS. Composition and Biological Activities of Ficus carica Latex. InFig (Ficus carica): Production, Processing, and Properties 2023; 597-641. Doi: 10.1007/978-3-031-16493-4_27
[5] El-Hawary SS, Ali ZY, Younis IY. Hepatoprotective potential of standardized Ficus species in intrahepatic cholestasis rat model: Involvement of nuclear factor-κB, and Farnesoid X receptor signaling pathways. Journal of Ethnopharmacology. 2019;231:262-74.Doi: 10.1016/j.jep.2018.11.026.
[6] Galati S, Di Stefano M, Martinelli E, Poli G, Tuccinardi T. Recent advances in in silico target fishing. Molecules. 2021;26(17):5124. Doi: 10.3390/molecules26175124.
[7] Lee A, Kim D. CRDS: consensus reverse docking system for target fishing. Bioinformatics. 2020;36(3):959-60. Doi: 10.1093/bioinformatics/btz656.
[8] Echeverry SM, Medina HI, Costa GM, Aragón DM. Optimization of flavonoid extraction from Passiflora quadrangularis leaves with sedative activity and evaluation of its stability under stress conditions. Revista Brasileira de Farmacognosia. 2018;28:610-7. Doi: 10.1016/j.bjp.2018.06.005.
[9] Eder J, Sedrani R, Wiesmann C. The discovery of first-in-class drugs: origins and evolution. Nature Reviews Drug Discovery. 2014;13(8):577-87. Doi: 10.1038/nrd4336.
[10] Su Y, Wang W, Wang Y, Wang C, Sun S, Zhu X, et al. Application and Development of Targeted Fishing Technology in Natural Product Screening-A Simple Minireview. Current Pharmaceutical Analysis. 2024;20(4):231-40. Doi: 10.2174/0115734129301241240429114323.
[11] Li H, Gao Z, Kang L, Zhang H, Yang K, Yu K, et al. TarFisDock: a web server for identifying drug targets with docking approach. Nucleic acids research. 2006;34(suppl_2):W219-W24.Doi: 10.1093/nar/gkl114
[12] Eldridge MD, Murray CW, Auton TR, Paolini GV, Mee RP. Empirical scoring functions: I. The development of a fast empirical scoring function to estimate the binding affinity of ligands in receptor complexes. Journal of computer-aided molecular design. 1997;11:425-45. Doi: 10.1023/a:1007996124545.
[13] Keiser MJ, Roth BL, Armbruster BN, Ernsberger P, Irwin JJ, Shoichet BK. Relating protein pharmacology by ligand chemistry. Nature biotechnology. 2007;25(2):197-206. Doi: 10.1038/nbt1284.
[14] Supino R. MTT assays. In vitro toxicity testing protocols. 1995:137-49. Doi: 10.1385/0-89603-282-5:137.
[15] Sayed MA, El-Rahman TMA, Abdelsalam H, Ali AM, Hamdy MM, Badr YA, et al. Attractive study of the antimicrobial, antiviral, and cytotoxic activity of novel synthesized silver chromite nanocomposites. BMC chemistry. 2022;16(1):39. Doi: 10.1186/s13065-022-00832-y.
[16] Liu C, Zou R, Mo F. Infrared Spectra Prediction for Functional Group Region Utilizing a Machine Learning Approach with Structural Neighboring Mechanism. Analytical Chemistry. 2024;96(39):15550-62. Doi: 10.1021/acs.analchem.4c01972.

Online ISSN: 3009-7800
Print ISSN: 3009-6324

[17] Zhu H, Clegg MS, Shoemaker CF, Wang SC. Characterization of diacylglycerol isomers in edible oils using gas chromatography–ion trap electron ionization mass spectrometry. Journal of chromatography A. 2013;1304:194-202. Doi: 10.1016/j.chroma.2013.06.058.
[18] Móricz ÁM, Baglyas M, Darcsi A, Balla J, Morlock GE. New Antioxidant Caffeate Esters of Fatty Alcohols Identified in Robinia pseudoacacia. Molecules. 2024;29(23):5673. Doi: 10.3390/molecules29235673.
[19] Liu X, Yu M, Chen J, Hu B, Huang J-B, Yang W-Q, et al. Anti-inflammatory 5, 6, 7, 8-tetrahydro-2-(2-phenylethyl) chromone derivatives from the stems of Aquilaria sinensis. Fitoterapia. 2024:106312. Doi: 10.1016/j.fitote.2024.106312.
[20] Milli G, Pellegrini A, Listro R, Fasolini M, Pagano K, Ragona L, et al. New LsrK Ligands as AI-2 Quorum Sensing Interfering Compounds against Biofilm Formation. Journal of Medicinal Chemistry. 2024;67(20):18139-56. Doi: 10.1021/acs.jmedchem.4c01266.
[21] Huynh T-H, Jang SC, Ban YH, Lee E-Y, Kim T, Kang I, et al. Discovery of Spirosnuolides A–D, Type I/III Hybrid Polyketide Spiro-Macrolides for a Chemotherapeutic Lead against Lung Cancer. Journal of the American Chemical Society. 2024. Doi: 10.1021/jacsau.4c00803.
[22] Cergol KM, Jensen P, Turner P, Coster MJ. Reversibility in the boron-mediated ketone–ketone aldol reaction. Chemical communications. 2007(13):1363-5. Doi: 10.1039/b617094c.
[23] Mabry T, Markham KR, Thomas MB. The systematic identification of flavonoids: Springer Science & Business Media; 2012. Doi: 10.1007/978-3-642-88458-0.
[24] Wahyuni I, Aulifa DL, Rosdianto AM, Levita J. Nephroprotective Activity of Angelica keiskei (Miq). Koidz. on Cisplatin-Induced Rats: Reducing Serum Creatinine, Urea Nitrogen, KIM-1, and Suppressing NF-kappaB p65 and COX-2. Drug Design, Development and Therapy. 2024:4707-21. Doi: 10.2147/DDDT.S481479.
[25] Singh P, Yadav S, Mahor AK, Singh PP, Bansal KK. Depiction of new flavonoids from Nyctanthus arbor-tristis, their antimicrobial activity and drug-likeness prediction. Natural Product Research. 2024:1-10. Doi: 10.1080/14786419.2024.2345757.
[26] Bello OM, Ogbesejana AB, Adetunji CO, Oguntoye SO. Flavonoids isolated from Vitex grandifolia, an underutilized vegetable, exert monoamine A & B inhibitory and anti-inflammatory effects and their structure-activity relationship. Turkish Journal of Pharmaceutical Sciences. 2019;16(4):437. Doi: 10.4274/tjps.galenos.2018.46036.
[27] Sakamoto Y. Flavones in Green Tea: Part III. Structure of Pigments IIIa and IIIb. Agricultural and Biological Chemistry. 1970;34(6):919-25. Doi:10.1080/00021369.1970.10859693.
[28] Jork H, Funk W, Fischer W, Wimmer H, Burns DT. Thin-layer chromatography. Reagents and detection methods. Physical and chemical detection methods: fundamentals, reagents I. Volume 1a. VCH, Weinheim, 1990 (ISBN 3-527-27834-6). xv+ 464 pp. Price DM 148.00. Analytica Chimica Acta. 1990;237:511-2. Doi: 10.1016/S0003-2670(00)83962-8.
[29] Gorin PA, Mazurek M. Further studies on the assignment of signals in 13C magnetic resonance spectra of aldoses and derived methyl glycosides. Canadian Journal of Chemistry. 1975;53(8):1212-23. Doi: 10.1139/v75-168.

Online ISSN: 3009-7800
Print ISSN: 3009-6324

[30] Österdahl, B. G., & Ankner, M. Chemical studies on bryophytes. 19. Application of 13C NMR in the structural elucidation of flavonoid C-glucosides from Hedwigia ciliata. Acta Chemica Scandinavica, 1978 32B(1), 93-97. Doi: 10.3891/acta.chem.scand.32b-0093.
[31] Che Zain MS, Shaari K, Lee SY, Fakurazi S. Development and Evaluation of Hydrogel-Thickened Nanoemulsion Containing Orientin, Isoorientin, Vitexin and Isovitexin as an Antioxidant Wound Dressing. Journal of Cluster Science. 2024;35(2):635-56. Doi: 10.1007/s10876-023-02504-w.
[32] Andersen OM, Markham KR. Flavonoids: chemistry, biochemistry and applications: CRC press; 2005. Doi:10.1201/9781420039443.
[33] Pereira CA, Yariwake JH, McCullagh M. Distinction of the C-glycosylflavone isomer pairs orientin/isoorientin and vitexin/isovitexin using HPLC-MS exact mass measurement and in-source CID. Phytochemical Analysis: An International Journal of Plant Chemical and Biochemical Techniques. 2005;16(5):295-301. Doi: 10.1002/pca.820.
[34] Pang S, Ge Y, Wang LS, Liu X, Lin CW, Yang H. Isolation and purification of orientin and isovitexin from Thlaspi arvense Linn. Advanced materials research. 2013;781:615-8. Doi: 10.4028/www.scientific.net/AMR.781-784.615
[35] Peng J, Fan G, Hong Z, Chai Y, Wu Y. Preparative separation of isovitexin and isoorientin from Patrinia villosa Juss by high-speed counter-current chromatography. Journal of Chromatography A. 2005 May 13;1074(1-2):111-5. Doi: 10.1016/j.chroma.2005.03.067
[36] Greenham JR, Grayer RJ, Harborne JB, Reynolds V. Intra-and interspecific variations in vacuolar flavonoids among Ficus species from the Budongo Forest, Uganda. Biochemical systematics and ecology. 2007;35(2):81-90. Doi: 10.1016/j.bse.2006.07.006.
[37] Ramadan MF. Fig (Ficus carica): Production, processing, and properties: Springer Nature; 2023. Doi: 10.1007/978-3-031-16493-4.
[38] Zafreen A, Mohamed MN, Islam S, Shamrin T, Abdiaziz AA, Rahman MA. Study of Phytochemical Screening and in vitro Antioxidant Activity of Ethanol Extract of Solanum sisymbriifolium leaf. Molecular Mechanism Research. 2024;2(1). Doi: 10.59429/mmr.v2i1.6742

Online ISSN: 3009-7800
Print ISSN: 3009-6324